Photoelectron spectroscopic and density functional theoretical studies of the 2′-deoxycytidine homodimer radical anion

Piotr Storoniak, Janusz Rak, Yeon Jae Ko, Haopeng Wang, and Kit H. Bowen

Citation: J. Chem. Phys. **139**, 075101 (2013); doi: 10.1063/1.4817779
View online: http://dx.doi.org/10.1063/1.4817779
View Table of Contents: http://jcp.aip.org/resource/1/JCPSA6/v139/i7
Published by the AIP Publishing LLC.

Photoelectron spectroscopic and density functional theoretical studies of the 2′-deoxycytidine homodimer radical anion

Piotr Storoniak,[1,a)] Janusz Rak,[1] Yeon Jae Ko,[2] Haopeng Wang,[2] and Kit H. Bowen[2,a)]
[1]*Department of Chemistry, University of Gdańsk, Wita Stwosza 63, 80-952 Gdańsk, Poland*
[2]*Department of Chemistry, Johns Hopkins University, Baltimore, Maryland 21218, USA*

(Received 11 May 2013; accepted 24 July 2013; published online 15 August 2013)

The intact (parent) 2′-deoxycytidine homodimer anion, $(dC)_2^{\bullet-}$, was generated in the gas phase (*in vacuo*) using an infrared desorption/photoemission source and its photoelectron spectrum was recorded using a pulsed, magnetic bottle photoelectron spectrometer. The photoelectron spectrum (PES) revealed a broad peak with the maximum at an electron binding energy between 1.6 and 1.9 eV and with a threshold at ∼1.2 eV. The relative energies and vertical detachment energies of possible anion radicals were calculated at the B3LYP/6-31++G** level of theory. The most stable anion radicals are the complexes involving combinations of the sugar · · · base and base · · · base interactions. The calculated adiabatic electron affinities and vertical detachment energies of the most stable $(dC)_2^{\bullet-}$ anions agree with the experimental values. In contrast with previous experimental-computational studies on the anionic complexes involving nucleobases with various proton-donors, the electron-induced proton transferred structures of $(dC)_2^{\bullet-}$ are not responsible for the shape of PES. © *2013 AIP Publishing LLC*. [http://dx.doi.org/10.1063/1.4817779]

I. INTRODUCTION

The interaction of ionizing radiation with biological systems results in secondary low energy electrons (LEEs) of energies in the range from 0 to 15 eV.[1] Because LEEs are shown to be capable of inducing strand breaks in dry DNA,[2] electron attachment to sub-units of DNA has been studied extensively in recent years.[3–16] Pyrimidines possess the highest electron affinities among the DNA constituents,[17] which suggests that both thymine and cytosine are plausible targets for thermalized electrons. Indeed, the gas phase adiabatic electron affinities (AEAs) of individual nucleobases predicted by different density functionals with different basis sets support the existence of valence bound (VB) anions of uracil, thymine, and possibly cytosine, but question the stability of the VB anions of purines.[18–20] Solvation increases the stability of the VB anions of nucleobases as indicated by the PES experiments of Hendricks *et al.*[21] and Schiedt *et al.*[22], the former of which demonstrated the existence of gas phase VB anions of canonical uracil solvated by a single atom of rare gas or water molecule. Analogous molecular anionic clusters were observed using the crossed beam RET (Rydberg Electron Transfer) technique against uracil and thymine anions solvated by rare gas atom.[23] Finally, the gas phase hydrogen-bonded complexes of nucleobases with various inorganic[24] and organic (alcohols, acids, amino acids)[25] proton donors were studied within joint PES-DFT studies, where an electron attachment induced barrier-free proton transfer was frequently observed.

The Watson-Crick AT[26–30] and GC[28,30–35] base pairs were also shown to form stable VB anions in the gas phase. The excess electron is localized on T or C in these complexes and the presence of a complementary purine base increases the AEA value of a pyrimidine.

Moving from the Watson-Crick AT and GC base pairs to the dA:dT and dG:dC nucleoside pairs, a significant increase in the electron affinity is observed. According to the B3LYP/DZP++ calculations, the gas phase AEAs for the dA:dT and dG:dC nucleoside pairs are 0.6 eV and 0.83 eV, respectively.[36,37]

The B3LYP/DZP++ approach was also used to study electron attachment to more complex DNA fragments like single-strand (dCpdG, dGpdC, dTpdA, dApdT, dGpdG, dGpdCpdG)[38–41] and double-strand nucleotide oligomers $(dGpdC)_2$).[42] Based on the theoretical estimates, all these systems easily accept the excess electron and form adiabatically stable radical anions.

The B3LYP/DZP++ calculations pertaining to 2′-deoxyribonucleosides predicted positive gas phase electron affinities for all of them. The theoretical AEA values of purine nucleosides are negligible (0.06 and 0.09 eV for dA and dG, respectively) compared to pyrimidine nucleosides (0.33 and 0.44 eV for dC and dT, respectively). However, the vertical detachment energy (VDE) value of 0.91 eV for dA (which is of similar magnitude to VDEs predicted for dC and dT) speaks in favor of the existence of the VB of 2′-deoxyadenosine anion radical in the gas phase.[43] Indeed, Stokes *et al.*[44] employing a combination of infrared desorption, electron photoemission, and gas jet expansion, recorded the anion photoelectron spectra of the nucleoside parent anions of 2′-deoxythymidine$^{\bullet-}$ ($dT^{\bullet-}$), 2′-deoxycytidine$^{\bullet-}$ ($dC^{\bullet-}$), 2′-deoxyadenosine$^{\bullet-}$ ($dA^{\bullet-}$), uridine$^{\bullet-}$ ($rU^{\bullet-}$), cytidine$^{\bullet-}$ ($rC^{\bullet-}$), adenosine$^{\bullet-}$ ($rA^{\bullet-}$), and guanosine$^{\bullet-}$ ($rG^{\bullet-}$). Their measurements proved the appearance of the stable valence radical anions of nucleosides in the gas phase. The experimental VDEs and AEAs of dT, dC, and dA match well with those calculated by Richardson *et al.*[43] and by Li *et al.*[45]

a)Authors to whom correspondence should be addressed. Electronic addresses: pondros@chem.univ.gda.pl and kbowen@jhu.edu

In the current work, we employ infrared desorption, electron photoemission, and a gas jet expansion to generate intact (parent anion) stable radical anionic species, (2′-deoxycytidine)$_2^{\bullet-}$, in the gas phase in order to record its photoelectron spectrum. In parallel, the B3LYP/6-31++G** calculations were carried out to elucidate the structure of the species responsible for the measured spectrum. The computational approach allowed us to identify the most stable radical anionic homodimers. The calculated VDEs for thermodynamically most favorable structures are in good agreement with the experimental values. We demonstrate that electron-induced barrier-free proton transfer does not occur in the VB (dC)$_2^{\bullet-}$ anions, which is in accord with our previous results for the nucleoside dimers, (rU)$_2^{\bullet-}$[46] and (dT)$_2^{\bullet-}$[47].

II. METHODS

A. Experimental details

2′-deoxycytidine radical dimer anions were generated using a novel pulsed infrared desorption-pulsed visible photoemission anion source which has been described previously.[44] Anion photoelectron spectroscopy (PES) is conducted by crossing beams of mass-selected negative ions and fixed frequency photons, followed by energy-analysis of the resulting photodetached electrons. This technique is governed by the energy conserving relationship: $h\nu = EBE + EKE$, where $h\nu$ is the photon energy, EBE is the electron-binding energy, and EKE is the measured electron kinetic energy.

Low-power infrared laser pulses (1.17 eV/photon) from a Nd:YAG laser were used to desorb neutral 2′-deoxycytidine from a slowly translating graphite rod which was thinly coated with the sample. Simultaneously, electrons were generated by visible laser pulses (another Nd:YAG laser operated at 532 nm, 2.33 eV/photon) striking a rotating yttrium oxide disk. Since yttrium oxide's work function of ∼2 eV is slightly below the photon energy of the visible laser, low energy electrons were produced, and this process is critical to the formation of intact (parent) biomolecular anions. At the same time a pulsed valve provided a collisionally cooled jet of helium to carry away excess energy and stabilize the resulting parent radical anions. The photoelectron spectrum of the intact 2′-deoxycytidine dimer radical anions was recorded by crossing a mass-selected beam of (dC)$_2^{\bullet-}$ parent anions with a fixed-frequency photon beam (a third Nd:YAG laser operated at 355 nm, 3.49 eV/photon). The photodetached electrons were energy-analyzed using a magnetic bottle energy analyzer with a resolution of 35 meV at EKE = 1 eV. Photoelectron spectra were calibrated against the well-known photoelectron spectrum of Cu^-.[48]

B. Computational details

Quantum chemical calculations were carried out by using density functional theory with Becke's three-parameter hybrid functional (B3LYP)[49–51] and the 6-31++G** basis set.[52,53] The usefulness of the B3LYP/6-31++G** method to describe intra- and intermolecular hydrogen bonds has been demonstrated through comparison with the second order Møller-Plesset (MP2) predictions for uracil · · · water complexes, which were treated at the MP2 level by van Mourik *et al.*[54] and at the B3LYP level by Harańczyk *et al.*[24(a)] Importantly, calculations at the B3LYP/6-31++G** level of Harańczyk *et al.* for the VB (uracil · · · water)$^-$ clusters reproduced very well the VDE value extracted from the photoelectron spectrum registered by Hendricks *et al.*[21] For these systems the B3LYP/6-31++G** results appeared as good as those calculated at the MP2/6-31++G(2df,2p)//MP2/6-311++G** level.[55]

Geometrical features of the 2′-deoxyribonucleosides obtained at the DFT level (torsional angles, bond lengths, valence angles, as well as intramolecular hydrogen bonds) were shown to correlate well with those obtained at the MP2 level.[56] Application of DFT and MP2 approaches also resulted in the identical energy order of the different conformers investigated in above reports.

The ability of the B3LYP method to predict excess electron binding energies was reviewed and the results were found to be satisfactory for valence-type molecular anions.[57]

All geometries presented here have been fully optimized without geometrical constraints, and the analysis of harmonic frequencies proved that all of them are also geometrically stable (all force constants were positive). The relative energies, ΔE, and Gibbs free energies, ΔG, of the neutral and anionic complexes are defined with respect to the energy of the most stable neutral or anionic configuration. The stabilization free energies, G_{stab}, of neutral complexes are calculated as a difference between the energy of the complex and the sum of the energies of fully optimized isolated monomers. In the case of anion radical complexes, G_{stab} are calculated by subtracting energies of the fully optimized anionic and neutral monomers from the energy of the given anion radical complex. The free energies of the neutral and anionic species result from correcting the relevant values of electronic energies for zero-point vibration terms, thermal contributions to energy, the pV term, and the entropy terms. These terms were calculated in the rigid rotor-harmonic oscillator approximation at T = 298 K and $p = 1$ atm.

The adiabatic electron affinity, AEA, is defined as the difference between the electronic energy corrected for zero-point energy of the neutral and the anion at their fully relaxed geometries. The vertical detachment energy, VDE, which is a direct observable in photoelectron spectroscopy experiment, is defined as the energy of neutral dimer minus the energy of the anionic dimer at the geometry of the fully relaxed anion. The vertical electron affinity, VEA, is the energy of the neutral minus the energy of the anion both at the fully relaxed neutral geometry.

All quantum chemical calculations have been carried out with the GAUSSIAN 03[58] and GAUSSIAN 09[59] codes. The pictures of molecules and molecular orbitals were plotted using the GaussView 4.1 program.[60]

III. RESULTS

A. Experimental results

Photoelectron spectrum of the 2′-deoxycytidine dimer radical anion is presented in Figure 1. A typical mass

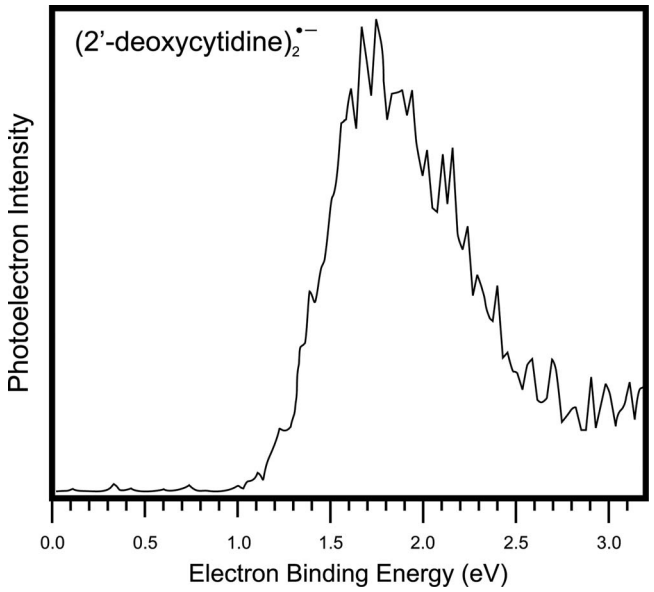

FIG. 1. Photoelectron spectrum of (2′-deoxycytidine)$_2^{\bullet-}$ recorded with 3.49 eV photons.

spectrum showing both the monomeric and dimeric anions of 2′-deoxycytidine is shown in the supplementary material as Figure S1.[61] The broad peak, indicative of a valence bound anion, results from the vertical photodetachment of the excess electron from a ground vibronic state of mass-selected nucleoside dimer radical anions to the ground vibronic state of the resulting neutrals. The maximal photoelectron intensities correspond to the optimal Franck-Condon overlaps of the vibrational wave functions between anion and neutral ground states. The photoelectron spectrum of (dC)$_2^{\bullet-}$ exhibits a broad peak covering the range of ∼1.2–2.5 eV. The maximum intensity of the signal, which occurs between 1.6 and 1.9 eV, corresponds to the experimental VDE value. The electron affinity (AEA) is more difficult to determine explicitly. Since there may be vibrational hot bands present in spectra such as these, the threshold EBE energy is not necessarily equivalent to the value of AEA. As a reasonable approximation, however, one can estimate the AEA value as that corresponding to the EBE at ∼10% of the rising photoelectron intensity. Therefore, from the onset of the photoelectron spectrum, AEA for (dC)$_2^{\bullet-}$ can be estimated to be ∼1.2 eV.

TABLE I. Values of relative electronic energy, free energy (ΔE and ΔG) for the conformations of the neutral and anion radical 2′-deoxycytidine, vertical detachment energies (VDEs), and adiabatic electron affinities (AEAs) of anion radical 2′-deoxycytidine calculated at the B3LYP/6-31++G** level. ΔE, ΔG are given in kcal/mol and VEA, AEA, and VDE are given in eV.

	Neutrals			Anions			
Conformation	ΔE	ΔG	VEA	ΔE	ΔG	AEA	VDE
C2′-endo/*anti*	−0.41	0.01	−0.15	0.14	1.75	0.25	1.14
C3′-endo/*anti*	0	0	−0.16	0	0	0.30	0.75

B. Computational results

The search through the dimer potential energy surface was preceded by the optimization of the neutral monomer. The starting nucleoside geometry was adopted after 2′-deoxycytidine nucleotide gas-phase PBE/aug-TZVP-GTH structure published by Smyth and Kohanoff.[62] Similar stability of the C3′-endo and C2′-endo sugar conformations[56] motivated us to take under consideration both neutral dC conformations, C2′-endo/*anti* and C3′-endo/*anti*. Figure 2 presents their B3LYP/6-31++G** optimized geometries. The C2′-endo monomer is more stable than C3′-endo by 0.41 kcal/mol, but this difference vanishes when the Gibbs free energies are compared (see Table I and Figure 2).

Both neutral conformations are characterized by almost identical negative vertical electron affinities (−0.15 and −0.16 eV). However, as indicated by the positive AEA values shown in Table I, the anion radicals should be stable once they are formed. The relative stability order of anions

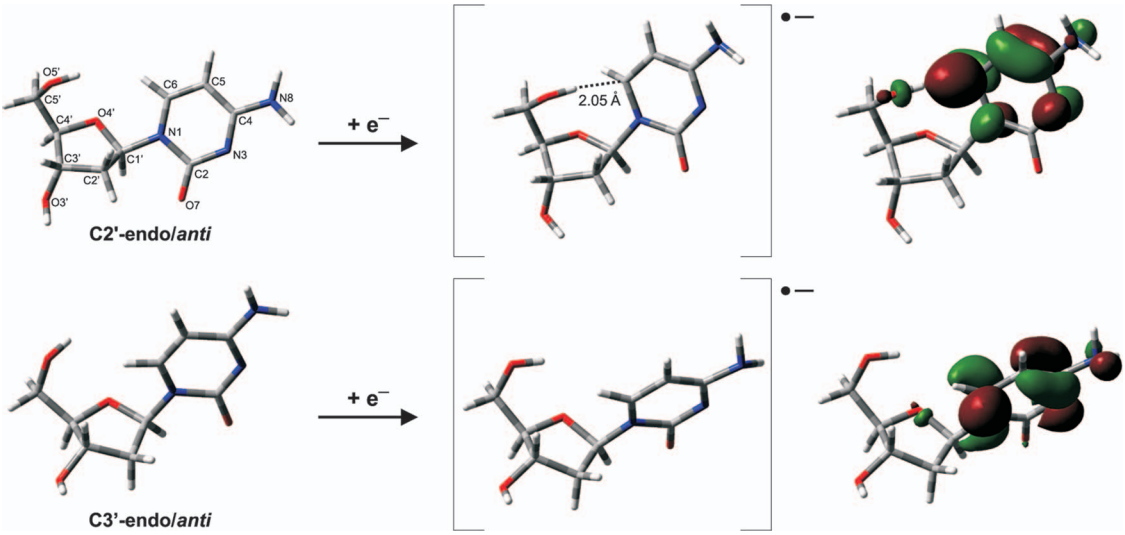

FIG. 2. Conformations of neutral and anion radical 2′-deoxycytidine monomers optimized at the B3LYP/6-31++G** level.

is reversed in comparison with the neutrals. The B3LYP/6-31++G** AEA values, 0.25 and 0.3 eV, agree with the computational value of 0.33 eV reported by Richardson *et al.*[43] and Li *et al.*[45] as well as with the experimental value, ∼0.5 eV, measured by Stokes *et al.*[44] There is a small difference in stability of the monomeric anion radicals compared to a significant difference of ∼0.4 eV in their VDE values (see Table I). As shown in Figure 2, the C2′-endo anion radical involves the intramolecular 5′O–H · · · C6 bond. This hydrogen bond presumably allows for better stabilization of the excess electron. The VDE calculated for the C3′-endo monomer matches perfectly its theoretical value of 0.72 eV calculated by Richardson *et al.*[43] and agrees well with the experimental VDE of 0.87 eV from the PES experiment.[44]

1. Structures and energetics of the neutral homodimers

The geometries of the neutral 2′-deoxycitidine homodimers optimized at B3LYP/6-31++G** level are shown in Figure 3. All 18 geometries were assembled from the optimized C3′-endo monomers discussed in the preceding section. Combination of the proton-donating centers (N8-H1, N8-H2, C5-H, O3′-H, O5′-H) with proton-accepting centers

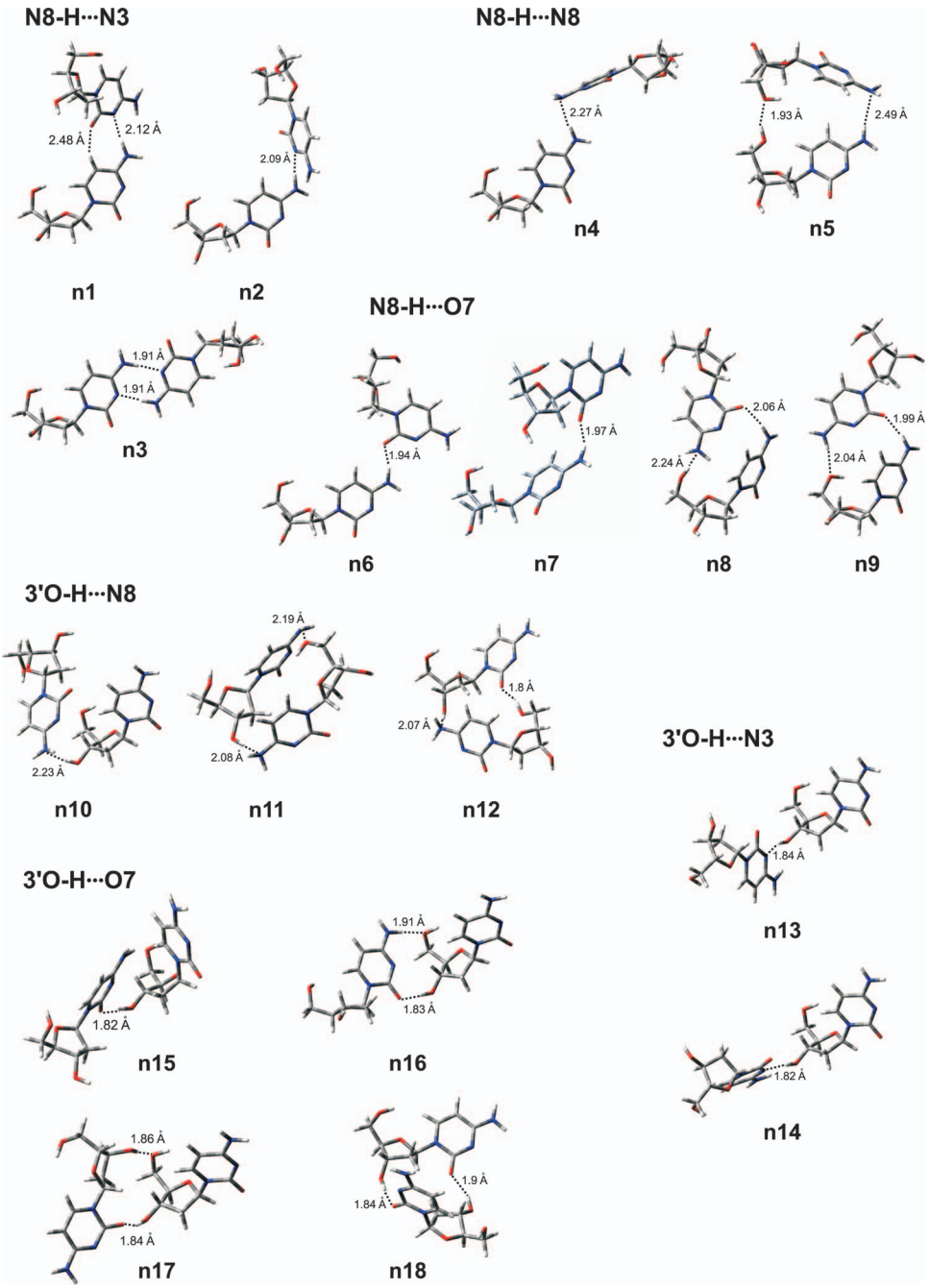

FIG. 3. Structures of neutral 2′-deoxycytidine homodimers optimized at the B3LYP/6-31++G** level.

TABLE II. Values of relative electronic energy and free energy (ΔE and ΔG) with respect to the most stable neutral 2′-deoxycytidine homodimer and stabilization free energies (G_{stab}) of the neutral 2′-deoxycytidine dimers calculated at the B3LYP/6-31++G** level. All values given in kcal/mol, VEA is given in eV.

Complex	ΔE	ΔG	G_{stab}	VEA
N8–H · · · N3 family				
n1	9.28	7.43	2.26	0.30
n2	9.09	7.94	2.77	0.24
n3	0.00	0.00	− 5.17	0.19
N8–H · · · N8 family				
n4	15.48	13.39	8.22	0.35
n5	10.93	11.67	6.50	0.27
N8–H · · · O7 family				
n6	8.44	6.28	1.11	0.28
n7	7.69	7.74	2.57	0.11
n8	8.93	10.99	5.82	0.31
n9	6.23	8.37	3.20	0.16
3′O–H · · · N8 family				
n10	9.95	11.78	6.61	0.31
n11	10.94	13.94	8.77	0.33
n12	5.73	8.71	3.54	0.20
3′O–H · · · N3 family				
n13	6.30	5.85	0.68	0.29
n14	5.99	6.03	0.86	0.22
3′O–H · · · O7 family				
n15	6.21	7.56	2.39	0.21
n16	2.58	4.51	− 0.66	0.27
n17	2.53	3.99	− 1.18	0.26
n18	1.02	3.13	− 2.04	0.13

(N8, O7, N3, O5′, O4′) leads to the structures stabilized through one or two hydrogen bonds. In Table II and Figure 3, the neutral $(dC)_2$ structures are organized according to their structural cognation.

As far as the relative orientation of the monomers is considered, the complexes can be divided into two main groups. A common feature of the complexes belonging to the first group (structures **n1**-**n9**) is the presence of a hydrogen bond involving the proton-donating N8-H site of one nucleobase and the proton accepting N3, N8, or O7 site of the second nucleobase. Within this family, there are dimers where, apart from the conventional hydrogen bonding solely among nucleobases, that is, N8-H · · · N3 (structures **n1-n3**), N8-H · · · N8 (**n4**), or N8-H · · · O7 (**n6**), interactions among the sugar and base (**n7-n9**) are also present, as well as the complex **n5**, in which the nucleosides are attracted to each other with base · · · base, N8-H · · · N8, and sugar · · · sugar, O5′-H · · · O5′, interactions.

In the second group of structures, the complexes are stabilized by sugar · · · base hydrogen bonds, that is, through interactions between the sugar's O3′-H proton donating site and the proton accepting atom of the cytosine moiety. There are complexes belonging to this family, where nucleosides interact via one or two hydrogen bonds, one of which being O3′-H · · · N8 (homodimers **n10-n12**), O3′-H · · · N3 (**n13, n14**), or O3′-H · · · O7 (**n15-n18**). As in the first group, apart from common (sugar)O3′-H · · · base bonding, in several complexes an additional hydrogen bond between sugar and base is formed (**n11, n12, n16-n18**).

The relative energies and Gibbs free energies (ΔEs and ΔGs), VEAs, as well as the stabilization free energies (G_{stab}s) calculated for each of the 18 neutral 2′-deoxycytidine homodimers are given in Table II. Their electronic energies and free energies span a wide range of values. The energy and free energy difference between the most (**n3**) and least (**n4**) stable structures is 15.5 and 13.4 kcal/mol, respectively.

The most stable are four homodimers, **n3**, **n18**, **n17**, and **n16**. The **n3** geometry belongs to the first group of structures while the three remaining belong to the second one. All these dimers are characterized by the negative G_{stab} values of −5.2, −2.0, −1.2, and −0.7 kcal/mol (see Table II), suggesting their occurrence in the gaseous dC. From the comparison of VEAs calculated for monomers and dimers it can be noted that homodimers should attach the excess electron more spontaneously than monomers, as indicated by the positive VEA values in Table II that span the range of 0.11 to 0.35 eV.

2. Structures and energetics of the anion radical homodimers

Our B3LYP/6-31++G** calculations ended up with 27 anion radical homodimers. All anionic structures are shown in Figure S2 in the supplementary material[61] and the most stable anion radicals are depicted in Figure 4. The thermodynamic characteristics of $(dC)_2^{\bullet -}$ complexes are gathered in Table III. The names of the anion radicals correspond to the names of the respective neutrals; for example, the anion radical denoted as **a1** originates from the geometry optimization of anion radical starting from the neutral **n1** geometry. This rule was applied to all geometries but the **a_N8H-O7/C5H-N3_intra**, **a_3′OH-N8**, and **a_3′OH-O7_intra** structures, where geometry optimization converged to the structures being far from the starting point. Therefore, the names of these three anions were supplemented with information on the intermolecular hydrogen bonds stabilizing the complex rather than on the neutral geometry they originated from. The suffix "intra" indicates structures, where an intramolecular, O5′H · · · C6, hydrogen bond is formed. Finally, the attachment of an electron to a given neutral $(dC)_2$ triggers, in some cases, intermolecular electron-induced proton transfer which is labeled by the "PT" suffix.

The most stable anionic complexes, **a13**, **a13_intra**, **a16_intra,** and **a8,** are displayed in Figure 4: the first three geometries differ no more than 0.7 kcal/mol in electronic energy while the last one is less stable by ∼1.2 kcal/mol than **a13**. The estimated adiabatic stability (AEA) for the most stable structures spans the range of ∼0.8–1.1 eV and for the structure **a13**, which is expected to dominate in the gas phase, AEA equals to 1.01 eV. Comparing the previously measured adiabatic affinities for 2′-deoxycytidine, which is ∼0.5 eV,[44] with the calculated value of 0.3 eV, one can assume that a +0.2 eV increment is necessary to convert the calculated value into a measured one. It is worth noting that the corrected AEA values for **a13** and for the remaining low energy dimeric anions match reasonably well with the experimental AEA of ∼1.2 eV measured for $(dC)_2^{\bullet -}$ in the present study (see Figure 1).

TABLE III. Values of relative electronic energy and free energy (ΔE and ΔG) with respect to the most stable 2′-deoxycytidine homodimer radical anion, stabilization free energies (G_{stab}), vertical detachment energies (VDEs), and adiabatic electron affinities (AEAs) of anion radical 2′-deoxycytidine homodimers calculated at the B3LYP/6-31++G** level. ΔE, ΔG, and G_{stab} are given in kcal/mol, AEA and VDE are given in eV.

Family	Complex	ΔE	ΔG	G_{stab}	AEA	VDE
3′O–H · · · N3	a13	0.00	0.00	− 14.77	1.01	1.60
3′O–H · · · N3	a13_intra	0.67	3.05	− 11.72	0.94	1.95
3′O–H · · · O7	a16_intra	0.68	3.84	− 10.93	0.79	1.79
N8–H · · · O7	a8	1.17	3.01	− 11.77	1.08	1.60
3′O–H · · · O7	a15	2.32	2.31	− 12.46	0.92	1.52
3′O–H · · · O7	a16	2.52	3.09	− 11.69	0.75	1.35
3′O–H · · · O7	a15_intra	2.77	3.48	− 11.29	0.87	1.88
3′O–H · · · O7	a17_intra	2.93	6.05	− 8.73	0.68	1.65
N8–H · · · O7	a_N8H-O7/C5H-N3_intra	3.58	3.84	− 10.94		1.86
3′O–H · · · N8	a10_intra	3.85	6.54	− 8.24	0.97	1.88
N8–H · · · N3	a1_intra	3.92	4.80	− 9.97	0.93	1.87
N8–H · · · N3	a1	4.07	2.81	− 11.97	0.96	1.50
3′O–H · · · O7	a18	4.20	5.72	− 9.05	0.60	0.88
N8–H · · · O7	a6	4.20	2.20	− 12.57	0.92	1.45
N8–H · · · N3	a3_PT	4.61	5.38	− 9.40	0.56	1.92
N8–H · · · N8	a5_intra	4.66	7.93	− 6.85	0.97	1.94
N8–H · · · N3	a3_intra_PT	5.25	6.12	− 8.65	0.51	2.20
3′O–H · · · N8	a12	5.38	7.09	− 7.69	0.77	1.38
N8–H · · · N3	a2	5.55	6.27	− 8.50	0.86	1.83
3′O–H · · · O7	a_3′OH-O7_intra	5.57	4.99	− 9.78		1.42
3′O–H · · · N8	a11	5.98	9.21	− 5.56	0.95	1.36
N8–H · · · N3	a3	6.53	4.17	− 10.61	0.52	0.60
N8–H · · · N3	a3_intra	7.59	7.92	− 6.85	0.43	1.40
N8–H · · · O7	a6_intra	7.73	8.61	− 6.16	0.75	1.88
N8–H · · · N3	a2_intra_PT	8.01	6.88	− 7.90	0.76	2.75
3′O–H · · · N8	a_3′OH-N8	11.50	8.57	− 6.21		1.12
N8–H · · · N8	a4_intra	13.52	12.78	− 2.00	0.80	1.66

The theoretical VDEs calculated for the structures of Figure 4 correlate perfectly with the maximum EBE, 1.6–1.9 eV, displayed on the photoelectron spectrum (see Figure 1). The highest VDE values among the most stable structures, 1.95 and 1.79 eV, are attributed to the **a13_intra** and **a16_intra** geometries, where one of the monomers features an intramolecular H-bond. As shown in Table I, the formation of the intramolecular O5′-H · · · C6 bond in

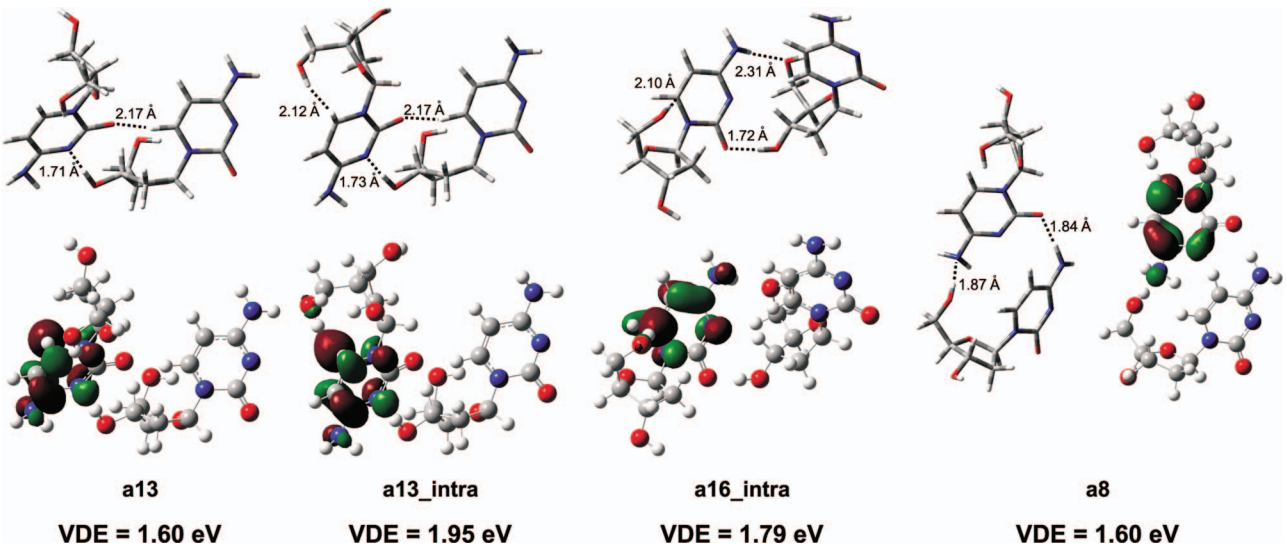

FIG. 4. Structures of the most stable anion radical 2′-deoxycytidine homodimers optimized at the B3LYP/6-31++G** level with corresponding VDE values and their singly occupied molecular orbitals plotted with a contour value of 0.05 $bohr^{-3/2}$.

2′-deoxycytidine monomer stabilizes the excess charge and shifts its VDE to higher values by 0.39 eV as compared to the nucleoside without an internal H-bond.

IV. DISCUSSION

The photoelectron spectrum recorded for $(dC)_2^{\bullet-}$ is experimental evidence of 2′-deoxycytidine's ability to exist in the gas phase as an adiabatically stable valence anion radical. The broad photoelectron spectral signal suggests that $(dC)_2^{\bullet-}$ may occur under our experimental conditions in several forms, these having various VDEs. This observation is in agreement with our results of quantum chemical modeling, which indicates that the four most stable structures possess almost identical energetic stability (Figure 4). These dimeric geometries are stabilized by two hydrogen bonds involving both sugars' and cytosines' sites. The H-bond pattern is identical in the two most stable anionic structures (**a13** and **a13_intra**). The only difference lies in the conformation of one of the nucleosides. Thus, **a13** and **a13_intra** are held together by the sugar · · · base, O3′-H · · · N3 and base · · · base, C6-H · · · O7 interactions. In the third most stable complex, **a16_intra**, one of the nucleosides utilizes two of the sugar's hydroxyl groups (its O3′-H serves as a proton donor and O5′ as a proton acceptor) to bind to the nucleobase of the second nucleoside. The least stable structure, **a8**, employs deoxyribose's 5′-end hydroxyl group as a proton donor to form a H-bond with the N8 of cytosine in the second nucleoside. The finding that the strongest stabilization of the anionic nucleoside dimer structures arises from the O3′-H · · · N3 sugar · · · base interaction agrees with our previous studies on the uridine and thymidine homodimer anions.[46,47]

Basically, two types of H-bonds that keep together the monomers in the studied dimers are discussed in the current paper as well as in Refs. 46 and 47. Namely, the H-bonds between nucleobases involves a proton acceptor site of one base and a proton donor site of another one. This type of complex forms the global minimum, **n3**, which is stabilized by two, N8-H · · · N3, such hydrogen bonds. To the another possible type of $(dC)_2$ belong the species which are stabilized by hydrogen bonds between the C3′-OH of one monomer and a proton acceptor site of cytosine in the second monomer. The most stable structure of this type is the **n18** dimer that is only 1 kcal/mol (ΔE) less stable than the **n3** one. Interestingly, the neutral global minimum does not support the most stable anion. Surprisingly, the favorable anionic structure is stabilized by only one hydrogen bond involving the C3′-OH proton donor site of one monomer. At the very first glance this finding is unintuitive. Electrostatic interactions between the charged and neutral monomer rather than hydrogen bonds may be responsible for the observed stability order of dimers. Probably, dipole · · · monopole interactions account for the observed effect. The direction of dipole moment in the dC molecule is shown in the supplementary material (see Figure S3).[61] Hence, the positive pole of dipole moment points to the region of negative charge in the **a13** and remaining anionic structures of the highest stability. The opposite arrangement is observed in the cytosine · · · cytosine geometries. As a consequence, attractive dipole · · · monopole interactions are present in **a13** while repulsive ones are present in the cytosine · · · cytosine families, which may explain the observed stability order. Similarly, in the least stable of anionic geometry, **a4_intra**, where monomers interact by single N8-H · · · N8 bond between cytosines', repulsive interactions between dipole and monopole are observed. An unfavorable dipole · · · dipole interaction between neutral nucleosides may already be noted in the neutral parent **n4** of the anionic homodimer **a4_intra**, which is the most unstable neutral homodimer among the considered geometries.

The VDE of 1.6 eV calculated for two of the four most stable anion radical complexes, **a13** and **a8**, shown in Figure 4, agrees with the lower limit of the EBE of the signal intensity maximum. Additionally, the remaining two complexes, **a13_intra** and **a16_intra**, may be responsible for the upper limit of the photoelectron signal at EBE of 1.9 eV.

Note that the thermodynamically most stable neutral complex, **n3**, stabilized by two N8-H · · · N3 H-bonds does not form the most stable anion radical (see **a3** in Table II). However, since electron induced proton transfer was shown to be an important stabilizing factor for anionic complexes involving nucleobases[24,25] we also modeled intermolecular proton transfer from N8H amine group to the N3 atom within anionic dimers originating from the most stable **n3** and the second most stable in the N8-H · · · N3 family **n2** geometry (see Table II). Three such anions, **a2_intra_PT**, **a3_PT**, and **a3_intra_PT**, have been identified and their characteristics as well as structures are gathered in Table III and Figure S2,[61] respectively. Despite favorable G_{stab} and AEA, we found these complexes to be relatively unstable in comparison to the lowest energy **a13** anion radical (see Table III). Moreover, the calculated VDEs 2.75 and 2.2 for dimers involving one monomer with intramolecular H-bond, **a2_intra_PT** and **a3_intra_PT**, respectively, are well above the measured vertical detachment energy (cf. Figure 1). Only a VDE of 1.92 eV obtained for the **a3_intra** complex, consisting of monomers without intramolecular H-bond, is close to the higher energy limit of maximum on the photoelectron spectrum (at ∼1.9 eV). Nevertheless, structure **a3_PT**, similar to remaining proton-transferred geometries, that is, **a2_intra_PT** and **a3_intra_PT**, is not expected to occur in the experiment due to its low stability.

The fact that thermodynamically most favorable neutral homodimers do not directly form the most stable anion radicals suggests that the formation of gaseous anionic dimer does not necessarily involve an electron attachment to the neutral dimer. In particular, it cannot be ruled out that the process leading to the formation of $(dC)_2^{\bullet-}$ starts from the attachment of electron to a monomeric nucleoside. Then the adiabatically stable (see Table I) $dC^{\bullet-}$ anion could interact with a neutral deoxycytidine molecule forming the anionic dimers observed in the photoelectron experiment.

Finally, we note that the maximum of photoelectron signal for the $(dC)_2^{\bullet-}$ anion is significantly shifted toward higher values of electron binding energy with respect to those of both the anionic cytosine dimer, $(cytosine)_2^{\bullet-}$,[63] and 2′-deoxycytidine, $(dC)^{\bullet-}$,[44] (see Figure 5). The vertical stability of 2′-deoxycytidine homodimer anion results from intermolecular interactions between the negatively charged

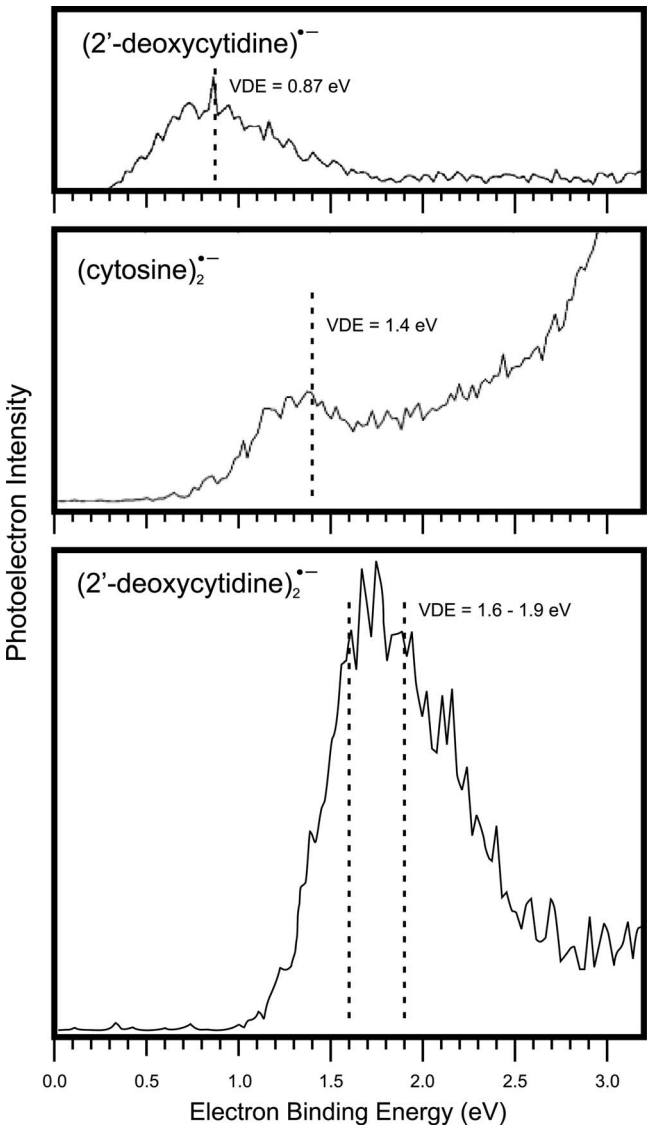

FIG. 5. Comparison of the anion photoelectron spectra of (2′-deoxycytidine)$^{\bullet-}$ from Ref. 44, (cytosine)$_2^{\bullet-}$ from Ref. 63, and (2′-deoxycytidine)$_2^{\bullet-}$ from the current study, recorded with 3.49 eV photons.

monomer and the neutral dC as well as from the presence of the sugar moiety in the anionic nucleoside. Hence, by comparing the vertical stability of (cytosine)$_2^{\bullet-}$ with that of the isolated cytosine anion radical, (cytosine)$^{\bullet-}$, one can estimate the effect of dimerization, while the comparison between the stability of (dC)$^{\bullet-}$ and (cytosine)$^{\bullet-}$ approximates the influence of the sugar moiety. The most accurate VDE for the cytosine valence anion amounts to 0.4 eV and originates from *ab initio* calculations carried out at the CCSD(T)/aug-cc-pVDZ level.[64] If one subtracts the computed VDE of 0.4 eV from the experimental VDE of 1.4 eV (see Figure 5) measured for cytosine homodimer, (cytosine)$_2^{\bullet-}$, one may draw the conclusion that intermolecular interactions present in the dimer shifts its VDE value by ∼1 eV toward higher EBEs. Comparing, in turn, the VDE of (cytosine)$^{\bullet-}$ to that of (dC)$^{\bullet-}$, which amounts to 0.9 eV (see Figure 5), one can estimate that the substitution of the N1 position of cytosine with the 2′-deoxyribose residue shifts the VDE value by ∼0.5 eV. On the premise that both effects are additive, supplementing VDE of isolated cytosine (0.4 eV) by the VDE shift of 1 eV (resulting from dimerization) and by 0.5 eV (the effect of the substitution of the N1 position of cytosine), one could estimate that the maximum of the photoelectron signal for (dC)$_2^{\bullet-}$ should be observed at EBE of ∼1.9 eV. The latter value matches relatively well the maximum of photoelectron spectrum reported herein.

V. CONCLUSION

The 2′-deoxycytidine homodimer anion (dC)$_2^{\bullet-}$ was investigated using a combination of anion photoelectron spectroscopy and computational approaches. The spectrum of the intact (dC)$_2^{\bullet-}$ exhibits a broad signal with a maximum located between EBE ∼ 1.6 and 1.9 eV and a threshold at EBE ∼ 1.2 eV. The value of the vertical detachment energy indicates strong stabilization of the nucleoside complexes. The significant width of the photoelectron spectral band suggests that more than one adiabatically stable valence bound anion may be populated under the experimental conditions. Taking into account possible configurations, we analyzed a number of homodimers involving the proton donor and acceptor centers of cytosine and sugar. The computational data obtained at the DFT level confirmed the existence of the stable valence anions of 2′-deoxycytidine dimers in the gas phase and gave insight into their structural and thermodynamic features.

We note that only a few of the considered neutral homodimer (dC)$_2$ configurations are thermodynamically viable, but all the considered configurations should readily accept the incoming electron (as indicated by their positive VEAs).

Due to a large number of dimer arrangements resulting from the possible combinations of proton donor and acceptor centers of the monomers, as well as due to the conformational flexibility of the nucleoside itself, we were able to study only a limited set of possible conformations. Nevertheless, our approach allowed us to interpret the photoelectron spectrum. The calculated VDEs indicate that we did identify the most important structures responsible for the experimentally observed picture.

The most stable anion radical homodimer, **a3**, turned out to be the complex where the nucleosides are connected by (sugar)O3′-H · · · N3(cytosine) and (cytosine)O7 · · · H-C6(cytosine) interactions. The second most stable conformer is stabilized by the same interactions as observed in **a3** and additionally possesses the internal hydrogen bond, 5′O-H · · · C6, within the anionic monomer.

ACKNOWLEDGMENTS

The experimental results reported here are based upon work supported by the National Science Foundation (NSF) under Grant No. CHE-1111693 (K.H.B.). This work was also supported by the Polish Ministry of Science and Higher Education (MNiSW), Grant No. DS/530-8221-D186-13 (J.R.). The calculations have been carried out at the Wrocław Center for Networking and Supercomputing (http://www.wcss.wroc.pl), under Grant No. 196 and at the Academic Computer Center in Gdańsk (TASK).

[1]S. M. Pimblott, J. A. LaVerne, and A. Mozumder, J. Phys. Chem. **100**, 8595 (1996).
[2]B. Boudaïffa, P. Cloutier, D. Hunting, M. A. Huels, and L. Sanche, Science **287**, 1658 (2000).
[3]B. Boudaïffa, P. Cloutier, D. Hunting, M. A. Huels, and L. Sanche, Radiat. Res. **157**, 227 (2002).
[4]M. A. Huels, B. Boudaïffa, P. Cloutier, D. Hunting, M. A. Huels, and L. Sanche, J. Am. Chem. Soc. **125**, 4467 (2003).
[5]F. Martin, P. D. Burrow, Z. Cai, P. Cloutier, D. Hunting, and L. Sanche, Phys. Rev. Lett. **93**, 068101 (2004).
[6]Y. Zheng, P. Cloutier, D. J. Hunting, L. Sanche, and J. R. Wagner, J. Am. Chem. Soc. **127**, 16592 (2005).
[7]Z. Cai, P. Cloutier, D. Hunting, and L. Sanche, J. Phys. Chem. B **109**, 4796 (2005).
[8]R. Panajotovic, F. Martin, P. Cloutier, D. Hunting, and L. Sanche, Radiat. Res. **165**, 452 (2006).
[9]Y. Zheng, P. Cloutier, D. J. Hunting, J. R. Wagner, and L. Sanche, J. Chem. Phys. **124**, 064710 (2006).
[10]Y. Zheng, J. R. Wagner, and L. Sanche, Phys. Rev. Lett. **96**, 208101 (2006).
[11]Z. Li, Y. Zheng, P. Cloutier, L. Sanche, and J. R. Wagner, J. Am. Chem. Soc. **130**, 5612 (2008).
[12]H. Abdoul-Carime and L. Sanche, Int. J. Radiat. Biol. **78**, 89 (2002).
[13]L. Sanche, Mass Spectrom. Rev. **21**, 349 (2002).
[14]X. Pan, P. Cloutier, D. Hunting, and L. Sanche, Phys. Rev. Lett. **90**, 208102 (2003).
[15]X. Pan and L. Sanche, Phys. Rev. Lett. **94**, 198104 (2005).
[16]J. Rak, K. Mazurkiewicz, M. Kobyłecka, P. Storoniak, M. Harańczyk, I. Dąbkowska, R. A. Bachorz, M. Gutowski, D. Radisic, S. T. Stokes, S. N. Eustis, D. Wang, X. Li, Y. J. Ko, and K. H. Bowen, "Stable valence anions of nucleic acid bases and DNA strand breaks induced by low energy electrons" in *Radiation Induced Molecular Phenomena in Nucleic Acid: A Comprehensive Theoretical and Experimental Analysis (Challenges and Advances in Computational Chemistry and Physics)*, edited by M. Shukla and J. Leszczynski, (Springer, 2008), pp. 619–667.
[17]M. Yan, D. Becker, S. Summerfield, P. Renke, and M. D. Sevilla, J. Phys. Chem. **96**, 1983 (1992).
[18]S. Wetmore, R. Boyd, and L. Eriksson, Chem. Phys. Lett. **322**, 129 (2000).
[19]N. Russo, M. Toscano, and A. Grand, J. Comput. Chem. **21**, 1243 (2000).
[20]S. Wesolowski, M. Leininger, P. Pentchev, and H. Schaefer, J. Am. Chem. Soc. **123**, 4023 (2001).
[21]J. H. Hendricks, S. A. Lyapustina, H. L. de Clercq, and K. H. Bowen, J. Chem. Phys. **108**, 8 (1998).
[22]J. Schiedt, R. Weinkauf, D. Neumark, and E. Schlag, Chem. Phys. **239**, 511 (1998).
[23]C. Desfrançois, V. Periquet, Y. Bouteiller, and J. P. Schermann, J. Phys. Chem. A **102**, 1274 (1998).
[24](a) M. Harańczyk, R. Bachorz, J. Rak, M. Gutowski, D. Radisic, S. T. Stokes, J. M. Nilles, and K. H. Bowen, J. Phys. Chem. B **107**, 7889 (2003); (b) Isr. J. Chem. **44**, 157 (2004).
[25]M. Harańczyk, J. Rak, M. Gutowski, D. Radisic, S. T. Stokes, and K. H. Bowen, J. Phys. Chem. B **109**, 13383 (2005); M. Harańczyk, I. Dąbkowska, J. Rak, M. Gutowski, J. M. Nilles, S. T. Stokes, D. Radisic, and K. H. Bowen, *ibid.* **108**, 6919 (2004); K. Mazurkiewicz, M. Harańczyk, M. Gutowski, J. Rak, D. Radisic, S. N. Eustis, D. Wang, and K. H. Bowen, J. Am. Chem. Soc. **129**, 1216 (2007); K. Mazurkiewicz, M. Haranczyk, P. Storoniak, M. Gutowski, J. Rak, D. Radisic, S. N. Eustis, D. Wang, and K. H. Bowen, Chem. Phys. **342**, 215 (2007); M. Gutowski, I. Dąbkowska, J. Rak, S. Xu, J. M. Nilles, D. Radisic, and K. H. Bowen, Eur. Phys. J. D **20**, 431 (2002); I. Dąbkowska, J. Rak, M. Gutowski, J. M. Nilles, D. Radisic, and K. H. Bowen, J. Chem. Phys. **120**, 6064 (2004); I. Dąbkowska, J. Rak, M. Gutowski, D. Radisic, S. T. Stokes, J. M. Nilles, and K. H. Bowen, Phys. Chem. Chem. Phys. **6**, 4351 (2004).
[26]N. A. Richardson, S. S. Wesolowski, and H. F. Schaefer, J. Phys. Chem. B **107**, 848 (2003).
[27]I. Al-Jihad, J. Smets, and L. Adamowicz, J. Phys. Chem. A **104**, 2994 (2000).
[28]A. Kumar, M. Knapp-Mohammady, P. C. Mishra, and S. Suhai, J. Comput. Chem. **25**, 1047 (2004).
[29]D. Radisic, K. H. Bowen, I. Dąbkowska, P. Storoniak, J. Rak, and M. Gutowski, J. Am. Chem. Soc. **127**, 6443 (2005).
[30]A.-O. Colson, B. Besler, D. M. Close, and M. D. Sevilla, J. Phys. Chem. **96**, 661 (1992).
[31]J. Smets, A. F. Jalbout, and L. Adamowicz, Chem. Phys. Lett. **342**, 342 (2001).
[32]N. A. Richardson, S. S. Wesolowski, and H. F. Schaefer III, J. Am. Chem. Soc. **124**, 10163 (2002).
[33]X. Li, Z. Cai, and M. D. Sevilla, J. Phys. Chem. B **105**, 10115 (2001).
[34]A. Szyperska, J. Rak, J. Leszczynski, X. Li, Y. J. Ko, H. Wang, and K. H. Bowen, J. Am. Chem. Soc. **131**, 2663 (2009).
[35]A. Szyperska, J. Rak, J. Leszczynski, X. Li, Y. J. Ko, H. Wang, and K. H. Bowen, Chem. Phys. Chem. **11**, 880 (2010).
[36]J. Gu, Y. Xie, and H. F. Schaefer, J. Phys. Chem. B **109**, 13067 (2005).
[37]J. Gu, Y. Xie, and H. F. Schaefer, J. Chem. Phys. **127**, 155107 (2007).
[38]J. Gu, Y. Xie, and H. F. Schaefer, Chem. Eur. J. **16**, 5089 (2010).
[39]J. Gu, Y. Xie, and H. F. Schaefer, Chem. Phys. Lett. **473**, 213 (2009).
[40]J. Gu, Y. Xie, and H. F. Schaefer, Chem. Eur. J. **18**, 5232 (2012).
[41]J. Gu, J. Wang, and J. Leszczynski, J. Phys. Chem. B **116**, 1458 (2012).
[42]J. Gu, N.-B. Wong, Y. Xie, and H. F. Schaefer, Chem. Eur. J. **16**, 13155 (2010).
[43]N. A. Richardson, J. Gu, S. Wang, Y. Xie, and H. F. Schaefer, J. Am. Chem. Soc. **126**, 4404 (2004).
[44]S. T. Stokes, X. Li, A. Grubisic, Y. J. Ko, and K. H. Bowen, J. Chem. Phys. **127**, 084321 (2007).
[45]X. Li, L. Sanche, and M. D. Sevilla, Radiat. Res. **165**, 721 (2006).
[46]Y. J. Ko, P. Storoniak, H. Wang, K. H. Bowen, and J. Rak, J. Chem. Phys. **137**, 205101 (2012).
[47]P. Storoniak, J. Rak, Y. Ko, H. Wang, and K. H. Bowen, J. Phys. Chem. B **116**, 13975 (2012).
[48]J. Ho, K. M. Ervin, and W. C. Lineberger, J. Chem. Phys. **93**, 6987 (1990).
[49]A. D. Becke, Phys. Rev. A **38**, 3098 (1988).
[50]A. D. Becke, J. Chem. Phys. **98**, 5648 (1993).
[51]C. Lee, W. Yang, and R. G. Parr, Phys. Rev. B **37**, 785 (1988).
[52]R. Ditchfield, W. J. Hehre, and J. A. Pople, J. Chem. Phys. **54**, 724 (1971).
[53]W. J. Hehre, R. Ditchfield, and J. A. Pople, J. Chem. Phys. **56**, 2257 (1972).
[54]T. van Mourik, S. L. Price, and D. C. Clary, J. Phys. Chem. A **103**, 1611 (1999).
[55]O. Dolgounitcheva, V. Zakrzewski, and J. Ortiz, J. Phys. Chem. A **103**, 7912 (1999).
[56]N. Foloppe and A. D. MacKerell, Biophys. J. **76**, 3206 (1999); A. Hocquet, N. Leulliot, and M. Ghomi, J. Phys. Chem. B **104**, 4560 (2000).
[57]J. C. Rienstra-Kiracofe, G. S. Tschumper, and H. F. Schaefer, Chem. Rev. **102**, 231 (2002).
[58]M. J. Frisch, G. W. Trucks, H. B. Schlegel *et al.*, GAUSSIAN 03, Revision B.05, Gaussian, Inc., Pittsburgh, PA, 2003.
[59]M. J. Frisch, G. W. Trucks, H. B. Schlegel *et al.*, GAUSSIAN 09, Revision B.01, Gaussian, Inc., Pittsburgh, PA, 2010.
[60]R. Dennington II, T. Keith, J. Millam, K. Eppinnett, W. Lee Hovell, and R. Gilliland, GAUSSVIEW, Version 3.09, Semichem, Inc., Shawnee Mission, KS, 2003.
[61]See supplementary material at http://dx.doi.org/10.1063/1.4817779 for mass spectrum showing both the monomeric and dimeric anions of 2′-deoxycytidine, complete anion radical homodimeric structures (listed in Table III) and the direction of dipole moment in the neutral 2′-deoxycytidine.
[62]M. Smyth and J. Kohanoff, J. Am. Chem. Soc. **134**, 9122 (2012).
[63]Y. J. Ko, H. Wang, R. Cao, D. Radisic, S. N. Eustis, S. T. Stokes, S. Lyapustina, S. X. Tian, and K. H. Bowen, Phys. Chem. Chem. Phys. **12**, 3535 (2010).
[64]X. Li, K. H. Bowen, M. Haranczyk, R. A. Bachorz, K. Mazurkiewicz, J. Rak, and M. Gutowski, J. Chem. Phys. **127**, 174309 (2007).